Nanoscale Organization of Chlorophyll *a* in Mesoporous Silica: Efficient Energy Transfer and Stabilized Charge Separation as in Natural Photosynthesis

Tetsuji Itoh,*,#,▽ Kazuhisa Yano,#,▽ Tsutomu Kajino,#,▽ Shigeru Itoh,† Yutaka Shibata,† Hiroyuki Mino,† Ryo Miyamoto,† Yuji Inada,‡ Satoshi Iwai,§ and Yoshiaki Fukushima#,▽

Toyota Central R & D Labs. Inc. and CREST, Japan Science and Technology Corporation, Yokomichi, Nagakute, Aichi 480-1192, Japan; School of Material Science (Physics), Graduate School of Science, Nagoya University, Furo-cho, Chikusa-ku, Nagoya 464-8602, Japan; Toin Human Science and Technology Center, Toin University of Yokohama, Kurogane-cho, Aoba-ku, Yokohama 225-8502, Japan; and Toyota Motor Corporation, Higashifuji Technical Center, 1200, Mishuku, Susono, Shizuoka, 410-1193, Japan

Received: May 31, 2004; In Final Form: July 8, 2004

Chlorophyll *a* molecules were adsorbed to mesoporous silica (FSM: folded-sheet mesoporous material) to form a chlorophyll−FSM conjugate capable of nanometer-scale interaction between chlorophyll *a* molecules as seen in a living plant leaf. The chlorophyll *a* molecules introduced into nanopores of FSM-22 (with a pore diameter of 4 nm) exhibited a red shift in the absorption peak and showed efficient excitation energy transfer from the shorter to the longer wavelength forms as characterized by the fast transient phase of 38 ps detected in the decay-associated spectrum (DAS) analysis of the fluorescence decay. Illumination of the chlorophyll−FSM-22 conjugate with visible light generated a stable chlorophyll *a* cation radical in the electron spin resonance (ESR) measurement, although the illumination of free chlorophyll *a* in solution produced almost no cation signal. The physiological function of the chlorophyll−FSM conjugate intercalated with ruthenium oxide (RuO_2) was explored as chlorophyll−FSM exhibited the photoinduced ability to catalyze the reduction of DCIP (an electron carrier). The mesoporous silica−chlorophyll conjugate in an appropriate system thus produced a solar energy conversion system enabling fast energy transfer and stable charge separation, presumably by producing the appropriate interaction of pigments as occurs in living photosynthetic apparatus.

Introduction

Hierarchical arrangements of molecular parts in the ordered nanoscale structure of living organs seem to be essential in realizing efficient biological system capabilities. Regulation of the molecular arrangements to accomplish the appropriate adjustments of the molecular interactions is indispensable for the design of efficient artificial energy conversion systems. The ordered arrangement of supramolecules, such as so-called J-aggregate-like BChl-c molecules (BChl-c consists of two parts; a Mg−porphyrin head moiety and a phytol hydrophobic tail chain) found in rod structures inside chlorosomes of green (non)sulfur bacteria,[1] has inspired many researchers to recreate the controlled molecular interactions and mimic the natural conjugates.[2,3] Rings formed by multiple BChl *a* molecules in the antenna LH2 protein[4] of purple photosynthetic bacteria suggest the suitable distance and mutual orientations between BChl *a* molecules, and seem to be essential for highly efficient energy transfer as well as stability of the structure under light illumination. Synthesis of artificial chemical compounds with architectures that mimic these structures for the purpose of accomplishing efficient energy transfer have been extensively attempted[5−7] Another approach, as in this study, aims at producing ordered arrangements of pigments by exploiting the molecular interactions. Nanoscale interactions between each BChl *a* molecule as well as with surrounding proteins are likely to be indispensable for the finetuning of pigment arrangements in the LH2 ring.[4] It is suggested that the interaction between pigment and surrounding molecules can be a new tool in molecular design of the artificial energy conversion assembly.

Recently, various types of mesoporous silica materials have been reported.[8,9] Their unique adsorption and catalytic activities have received much attention.[10−17] Nanoscale spaces in pores inside silica and the adsorbing forces of the silica surfaces are expected to play a special role in organizing the supramolecules adsorbed inside the pores, such as the proteins in biological systems. We report here the formation of photostable chlorophyll−FSM conjugates due to the interaction between chlorophyll molecules inside the mesoporous spaces of FSM.[18,19] In Table 1,[18] properties of chlorophyll−FSM conjugates are listed. It is noteworthy that an increase in the pore diameter of FSM is accompanied by a shift of the absorption maximum to a longer wavelength, and also by enhancement of the photostability of the chlorophyll−FSM conjugate. These results suggest that enhancement of the photostability of chlorophyll in conjugates is accompanied not only by the interaction between chlorophyll and the supporting silica materials, but also by the interaction between neighboring chlorophyll molecules. Furthermore, the chlorophyll−FSM conjugate catalyzes photoreduction and hydrogen gas evolution under visible light.[19] However, the mechanism for these abilities and structural information regarding the pigment arrangement inside the pores have not yet been clarified. We suggest that the special abilities of the conjugate

* Corresponding author. Present address: National Institute of Advanced Industrial Science and Technology (AIST**),** Nigatake 4-2-1, Miyanogino-ku, Sendai, 983-8551, Japan, Phone: (+81)22-237-3097, FAX: (+81)22-237-5226, E-mail: t-itoh@ni.aist.go.jp.

Toyota Central R & D Labs. Inc.

▽ CREST, Japan Science and Technology Corporation.

† Nagoya University.

‡ Toin University of Yokohama.

§ Toyota Motor Corporation.

10.1021/jp047661t CCC: $27.50
Published on Web 08/14/2004

TABLE 1: Physicochemical and Spectrophotometric Properties of Chlorophyll−FSM Conjugates

	compound pore diameter (nm)	chlorophyll *a* adsorbed (mg/100 mg FSM)	absorption maximum (nm)	stablization of chlorophyll *a* (%)*
FSM-22	4.0	29.2	677	100
FSM-16	2.7	24.6	675	97
FSM-14	2.4	15.8	673	52
FSM-10	1.6	0.75	670	50
chlorophyll *a* in benzene			665	<8
chlorophylls in intact leaves			678	100

*Relative value of absorbance at absorption maximum in the red region after 360 min illumination. The absorbance value of each sample obtained before the irradiation was regarded as 100%.

are probably due to the stabilized energy or electron-transfer abilities arising from the interaction between guest molecules in the pores of host materials.

The present study deals with the chlorophyll aggregates formed in the mesoporous silica pores of suitable pore sizes and their organization that facilitates the photochemical activity of charge separation and energy transfer.

Experimental Section

General. Chlorophyll *a* was purified from *Spirulina* purchased from Wako Pure Chemical Industries, Ltd. (Osaka, Japan) The mesoporous materials, FSM-10 and FSM-22 materials, with pore diameters of 1.6 and 4.0 nm, respectively, were prepared from kanemite (layered polysilicate) using alkyltrimethylammonium [$C_nH_{2n+1}N^+(CH_3)_3$] with different alkyl-chain lengths ($n = 10$ and 22), according to the method reported by Inagaki et al.[8]

Chlorophyll−FSM-10, -22 Conjugates. Two types of conjugates, chlorophyll−FSM-10 and -22 conjugates, were prepared by the method of Itoh et al.[18] to test whether the chlorophylls in FSM pores cause energy transfer. In previous studies, we found that only a small amount of chlorophyll molecules was adsorbed to FSMs with pore sizes of less than 2 nm. On the other hand, more than 10 wt % of chlorophyll was adsorbed *into* FSMs with larger pore sizes (Table 1).[17] The more chlorophyll adsorbed, the higher the photostability of the conjugates. The higher stability probably resulted from the more efficient energy and electron-transfer abilities between chlorophyll molecules. We used two types of host materials; FSM-10 and -22, which have the smallest (pore diameter of 1.6 nm) and largest pore sizes (pore diameter of 4 nm), respectively, among the materials listed in Table 1.

Preparation of Chlorophyll−FSM-22−RuO_2. Ruthenium oxide, RuO_2, incorporated into Chlorophyll−FSM-22, was prepared to test whether the conjugate catalyzes photoreduction of DCIP (*2, 6, dichlorophenolindophenol sodium salt*) by visible light. First, an aqueous solution (3 mL) of ruthenium chloride (III) (18 mg) was added to powdered FSM-22 (500 mg), and the mixture was dried under pressure at 40 °C. After heating at 400 °C in the presence of N_2 and O_2 (N_2: 900 mL/min, O_2: 100 mL/min), the FSM-22−RuO_2 was suspended in a 0.1% NaOH methanol solution for 3 min to prepare Na−FSM-22−RuO_2. The resulting product was filtered, washed with methanol, and then air-dried at 45 °C. Na−FSM-22−RuO_2 (100 mg) was added to 4.0 mL of chlorophyll *a* dissolved in benzene (10 mM). The suspension was then shaken for 30 min at 25 °C to establish an adsorption equilibrium.[19]

Photoreduction of DCIP (2, 6, dichlorophenolindophenol) by Chlorophyll−FSM-22−RuO_2. The photoreduction of DCIP was examined in the absence of a donor. The conjugate (30 mg, 3.4 μmol as chlorophyll) was suspended in 10 mL of 100 mM Tris-HCl buffer (pH 10) containing 0.05 mM DCIP. The sample in the cell was illuminated with a 500 W xenon lamp (light intensity, 380 J m^{-2} s^{-1}). Light wavelengths of less than 400 nm were blocked with a Toshiba L-39 filter (Tokyo, Japan). The amount of reduction of DCIP was spectrophotmetrically observed by measuring the absorbance at 600 nm of the supernatant liquor of the sample suspension after centrifuging, using the molar extinction coefficient of 2.06×10^4 M^{-1} cm^{-1}.

Characterization of Energy Transfer by the Measurements of Fluorescence Lifetime. Time-resolved fluorescence spectra and fluorescence decay time courses were measured using a streak camera system (Hamamatsu Photonics, C4334 Streakscope) operated in a photon-counting mode. The sample was excited at 630 nm by a pulsed laser diode synchronously flashing at a repetition frequency of 1 MHz with pulse duration of ~50 ps, which limits the time-resolution of the system to around 10 ps after deconvolution. The powdered Chl *a*−FSM conjugates were pasted on the surface of cover glass, and contained in a liquid N_2 cryostat (Oxford, DN1704). The sample fluorescence was focused on the entrance slit of a 50-cm monochromator through a long-pass filter (>640 nm) to eliminate the excitation pulse. The wavelength-dispersed fluorescence was then time-resolved by a streak scope. The wavelength−time 2D profile of the fluorescence was obtained as a CCD camera image (640 × 480 pixels) as described elsewhere. The typical accumulation time of fluorescence for each measurement was about 1 h. The ESR spectrum was measured at room temperature with a Bruker (Rheinstetten, Germany) ESP300 spectrometer operating at 9.78586 GHz.

Results and Discussion

Time-resolved Fluorescence Spectra of Chlorophyll−FSM-22 and Chlorophyll−FSM-10. As listed in Table 1, the Chl *a*-FSM conjugate with a large pore size shows a red-shifted absorption peak for Chl *a* with a broader bandwidth tailed to the longer wavelength side. We examined whether the chlorophylls inside each pore of FSM show energy transfer between each other, by means of the ps streak camera fluorescence measurement system. Figure 1a shows the wavelength−time image of fluorescence decay and the time-resolved fluorescence spectra of chlorophyll−FSM-22 (which contains 23 mg chlorophyll *a*/100 mg FSM) obtained with 620-nm excitation. The latter spectra were normalized to the maximum intensity of each spectrum. Within the first 0−1 ns, the fluorescence of chlorophyll showed a peak at 760 nm. The peak subsequently shifted to the longer wavelength, and finally showed a peak at around 800 nm. It is noteworthy that the shift of the fluorescence band to the longer wavelength side became more prominent with an increase in the pore diameter of FSM. The shift of the fluorescence band seems to be attributable to the presence of the longer wavelength form of chlorophyll *a* as a minor component. The longer wavelength form seems to be produced due to the stronger interaction between the chlorophyll molecules, presumably in a packed arrangement of the pigments as postulated in Scheme 1a. The component can be detected

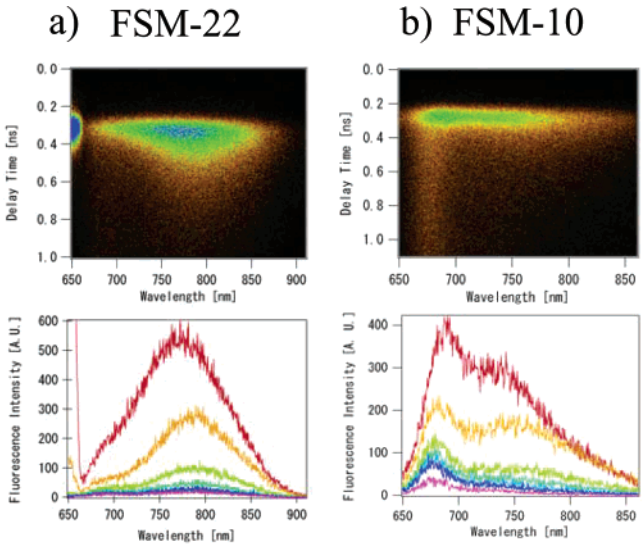

Figure 1. Wavelength−time two-dimensional image of fluorescence decay after the 50 ps laser excitation. Images of fluorescence and the time-resolved fluorescence spectra of chlorophyll−FSM-22(A) and chlorophyll−FSM-10(B) were obtained by excitation at 620 and 405 nm, respectively. The time origin in the images is set at the peak of the excitation laser pulse. Time-resolved fluorescence spectra were calculated every 140 ps and are displayed in the lower figures.

SCHEME 1

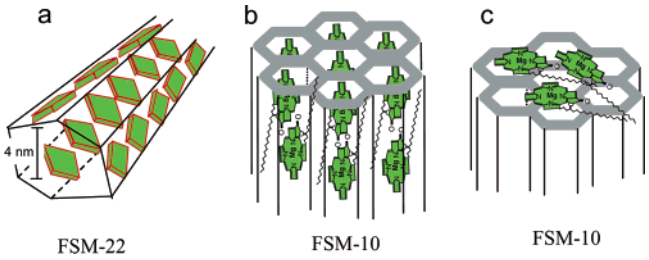

only as the longer-wavelength tail in the absorption spectrum, but shows as a prominent peak in the time-resolved fluorescence spectrum. The arrangement of the chlorophyll molecules responsible for the longer-wavelength fluorescence might be similar to those detected in the photosystem I reaction center of green plants that usually gives a fluorescence peak at around 725−750 nm. It is suggested that the arrangement of chlorophyll molecules inside each nanoscale pore of chlorophyll−FSM-22 resembles those in light-harvesting or reaction-center complexes of living plants, that is, exhibiting red-shifted spectral forms and fast energy transfer. The fluorescence of chlorophyll−FSM-10 (100 mg, 0.75 mg as chlorophyll *a*) showed two peaks at 690 and 740 nm, respectively. It seems that the 690-nm form does not transfer energy to the 740-nm form, since the lifetime of the former was longer than that of the latter. The two spectral forms might represent two types of chlorophyll aggregates inside or outside the FSM (Schemes 1b and 1c). These two forms seem to exist too far apart to allow efficient energy transfer. The peak positions of the fluorescence of chlorophyll−FSM-10 did not change with decay time.

Fluorescence decay kinetics of chlorophyll−FSM-22 at 77 K were further analyzed with an excitation wavelength at 620 nm to excite predominantly monomeric chlorophyll molecules. Decay-associated spectra calculated from Figure 1 image-data are shown in Figure 2. The 38-ps-time constant energy transfer component, characterized by the positive amplitudes in the 665−760 nm region (loss of excitation energy) and the negative amplitudes in the 760−850 nm regions (gain of excitation

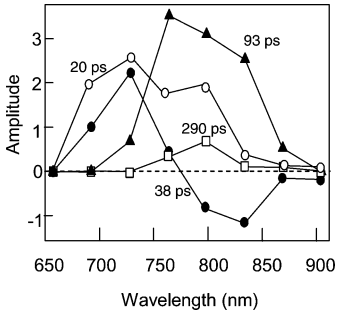

Figure 2. Decay-associated fluorescence spectra of chlorophyll−FSM at 77 K calculated from images such as that in Figure 1. The wavelength-decay images were divided into eight wavelength regions. The fluorescence decay curves in each region were integrated along the wavelength. The eight fluorescence decay curves, thus obtained, were fitted by a sum of 3−5 exponential functions convoluted with a Gaussian instrumental function using the nonlinear least-squares fitting algorithm in IGOR PRO (Wave Metrics). Initially, the data curves were fitted without any constraint. The data were then fitted using the global fitting algorithm in which the time constants were shared among the eight decay curves. According to this procedure, we obtained the decay-associated spectra (DAS), which are the preexponential factors for the same time constants plotted as a function of wavelength.

energy) were assigned to the energy transfer from the high energy chlorophyll forms to the red-shifted low-energy chlorophyll forms. The other components (20, 93, and 240 ps) showed only positive peaks, suggesting simple decay without donating energy to other components. The exponential decays of the excitation energy transfer processes are in line with the previous measurements obtained from the single photon counting method.[20] The area under the amplitude curve is remarkably larger for the positive high-energy chlorophyll fluorescence than for the low-energy chlorophyll fluorescence around 850 nm as reported for natural chlorosomes.[21] Very fast excitation energy transfer from the high energy chlorophyll forms in just a few ps was also suggested from the time-resolved spectra at the rising edge of the fluorescence, but its time constant could not be resolved clearly. In addition to the energy transfer components, Figure 2 also displays trapping components of 93 and 290 ps, which each suggest the decay of equilibrated pools of high and low energy chlorophyll forms. The high-energy chlorophylls seem to be quenched by the neighboring low-energy chlorophylls through the 38-ps energy transfer in the case of the chlorophyll−FSM-22 conjugate (Scheme 1). In the pores of FSM-22, chlorophylls seem to self-aggregate to form oligomers with longer wavelength absorption peaks through strong pigment−pitment interaction. The lifetime of fluorescence of low-energy chlorophylls was shorter than that of bulk chlorophylls in the solution (around 6 ns, data not shown). The fast decay time suggests the existence of fast nonradiative decay processes of excitation energy in the low-energy chlorophylls. The fast decay, therefore, seems to explain why not only energy transfer, but also efficient electron transfer, occurs in the chlorophyll−FSM-22 conjugate only, and not in the chlorophyll−FSM-10 conjugate chlorophyll powders as described below.

Charge Separation on the Chlorophyll−FSM-22 Conjugates. Generation of the chlorophyll cation radical of chlorophylls in chlorophyll−FSM-22 conjugates was measured using a CW electron spin resonance (ESR) method under light illumination, as shown in Figure 3. Formation of free radicals in chlorophyll−FSM-22 powder ($g = 2.003\ 25$) and chlorophyll powder ($g = 2.002\ 53$) was seen. These radicals seem to represent cation radicals of chlorophyll *a* since g-values of chlorophyll cation radicals are known to be around $g = 2.003$ in plant materials.[22] Upon the illumination of chlorophyll−FSM-

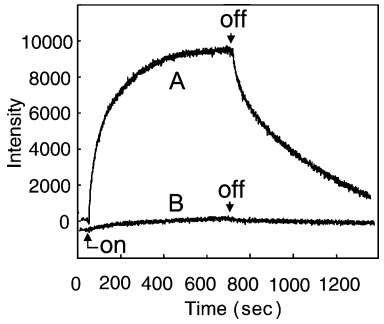

Figure 3. Generation of chlorophyll cation radicals in the chlorophyll−FSM conjugates under illumination with white light. The amount of generated chlorophyll cation radicals is represented by the peak intensity at 3486.6 or 3483.9 G. Curve A: chlorophyll−FSM-22 conjugate (at a chlorophyll content of 2.2×10^{-6} mol). Curve B: chlorophyll powder (at 1.2×10^{-5} mol).

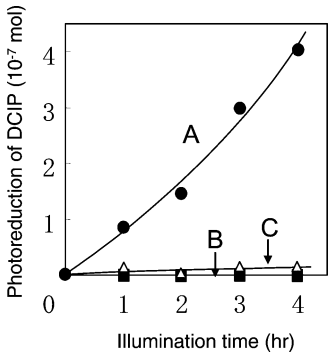

Figure 4. Photoreduction of DCIP by Chl−FSM-22−RuO_2 (light intensity: 380 J m^{-2} s^{-1}) at 30 °C. Light wavelengths less than 400 nm were blocked with a Toshiba L-39 filter (Tokyo, Japan). Curve A: Reaction system (10 mL) consisting of Chl−FSM-22−RuO_2 (30 mg) and DCIP (0.05 M). Curve B: Same as for Curve A, but with FSM-22−RuO_2 (30 mg) substituted for Chl−FSM-22−RuO_2. Curve C: Chl−FSM-22−RuO_2 (30 mg) and DCIP (0.05 M) in the dark.

22 powder with white light, the extent of the free-radical signal increased with illumination time, suggesting the occurrence of an electron transfer process inside the pores of FSM-22 (curve A). When the light was turned off, the radical intensity decreased very slowly biphasically with apparent decay time constants of 1−5 and 400 s, respectively. Radicals existed to some extent for several tens of minutes, indicating that the chlorophyll cation radicals produced in the pores of FSM are very stable. Radical formation in chlorophyll powder was almost negligible, (curve B) indicating that the charge separation efficiency in the chlorophyll−FSM-22 conjugate is significantly high and stable.

Attempts to achieve long-lived charge separation have been made using various organic compounds that combined chlorophylls with electron acceptor molecules held in well-defined geometries. A system with efficient capture of light energy, fast excitation transfer inside the antenna moiety to the reaction center moiety, and rapid stable charge separation in the reaction center moiety has been the aim of attempts to produce an analogy to the natural photosynthesis system. Here, we have presented a simple but efficient chlorophyll−FSM conjugate system that enables efficient energy capture, fast energy transfer among chlorophylls with different energy levels, capture of excitation energy in the charge separation, and high stabilization of the charge-separated-state radical. The system contrasts strongly with chlorophyll powder, which produced almost no chlorophyll cation radicals. Although the electron acceptor has not been added to this system, radical formation was clearly detected. The acceptor in the present system has not yet been clarified, but it is likely to be oxygen in the FSM pores. To confirm this point, photoreduction of nitro blue tetrazolium (NBT, 0.75 mM) by chlorophyll−FSM conjugate was tested in the presence and absence of superoxide dismutase (SOD, 100 units) according to the method of Itoh et al.[23] The photoreduction proceeded under illumination, but was decreased by the addition of SOD (data not shown). Therefore, the photoreduction of NBT depends on a superoxide anion that is probably generated by the action of the photoexcited chlorophyll−FSM conjugate and diffused out of the pores, because SOD is too large to intercalate into the pores. We have reported the high photostability of the chlorophyll−FSM conjugate and have suggested that it is due to the interaction between chlorophyll molecules inside the mesoporous space of FSM. The conjugate also catalyzes photoreduction of hydronium ions and produces hydrogen gas when illuminated with visible light.[19] As mentioned above, the chlorophyll−FSM conjugate provides an efficient light-harvesting system with inclined energy levels of chlorophylls in excited states and undergoes charge separation into red chlorophylls at

SCHEME 2

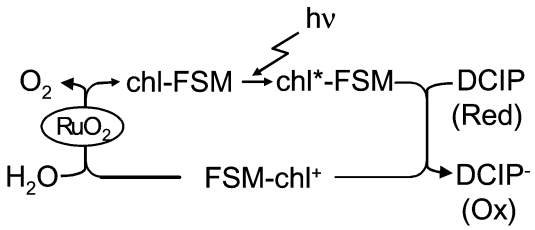

DCIP:2, 6, dichlorophenolindophenol sodium salt

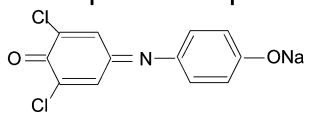

the reaction center. Synthesis of a self-organized supramolecular machine that collects light energy for electron transfer has been achieved by the use of FSM nanopores.

Photoreduction of DCIP (2, 6, dichlorophenolindophenol) by Chlorophyll−FSM-22−RuO_2. Figure 4 shows the photoreduction of DCIP by chlorophyll−FSM-22−RuO_2 and FSM-22−RuO_2. The photoreduction of DCIP by chlorophyll−FSM-22−RuO_2 was enhanced linearly by increasing the illumination time, as shown by curve A. On the other hand, no reduction of DCIP by FSM-22−RuO_2 under illumination or chlorophyll−FSM-22−RuO_2 in the dark was observed (curves B and C). As shown by curve A, approximately 0.4 μmol of reduced DCIP was generated in 4 h, at which time the reaction was still progressing. This indicates that the amount of reduced DCIP was 10 times greater than the amount of chlorophyll cation radicals (approximately 0.04 μmol) in the reaction system. Since the standard oxidation−reduction potential of DCIP is 0.217 V,[24] a photoreduction system containing chlorophyll−FSM-22−RuO_2 can probably be expected to oxidize water into oxygen molecules. Based on the results described above, the chlorophyll conjugate excited by illumination (Chl*−conj.) releases an electron, thereby changing into a cationic chlorophyll conjugate (Chl^+−conj.). The electron reduces DCIP. On the other hand, the Chl^+−conjugate oxidizes water to oxygen gas through the catalytic action of RuO_2 (Scheme 2). We have described how photostable chlorophyll−FSM conjugate supports the interaction between chlorophyll molecules in the mesopore spaces of FSM. This conjugate catalyzes photoreduction and hydrogen gas evolution under visible light.[19] As suggested above, the light-harvesting system in chlorophyll−FSM is a supramolecular machine that collects light energy for electron transfer.

Arrangements of Chlorophylls Inside the FSM Nanopore. In our previous study,[18,19] we introduced chlorophyll molecules into the nanospaces of mesoporous silica, and confirmed the energy and electron transfer in an arrangement comparable to the self-organized assembly of chlorophylls in the photosynthetic apparatus of living organisms. The chemical structure of chlorophyll *a* consists of two parts: a Mg−porphyrin head moiety and a phytol hydrophobic tail chain. Both moieties are expected to interact with solvents and the silica surfaces in different ways, and are likely to control the adsorption and self-organization of chlorophylls inside mesoporous silica. The arrangement of chlorophylls and the distance between the porphyrin rings are important in determining the molecular interaction that leads to the changes in the absorption/fluorescence peak, energy transfer efficiency, and charge separation probability. The orientation and interring distances seem to be regulated by the pore-size of the mesoporous silica. Different types of interaction seem to occur among chlorophyll aggregates inside the mesoporous silica with suitable pore size, resulting in efficient stable photochemical activity. The physicochemical properties of silica itself seem also to be important to achieve high adsorption and well-organized molecular interactions. The silica nanoporous material thus provides the environment to attain both the great photostability[18,19] of the conjugates and the highly efficient photoreaction described in this study. We believe that chlorophyll molecules conjugated with well-designed multilayered nanoporous compounds will create a new breakthrough for artificial photosynthesis.

References and Notes

(1) Blankenship, R. E.; Olson, J. M.; Miller, M. In *Anoxygenic Photosynthetic Bacteria*; Blankenship, R. E., Madigan, M. T., Bauer, C. E. Eds. Kluwer Academic Publishers: 1995; pp 413−418.

(2) Smith M. K.; Kehres A. L.; Fajer J. *J. Am. Chem. Soc*. **1983**, *105*, 1387−1389.

(3) Krasnovsky A. A.; Bystrova M. I. *Biosystems* **1980**, *12*, 181−194.

(4) Papiz, M. Z.; Cogdell, R. J.; Isaacs, N. W. *Nature* **1995**, *374*, 517−521.

(5) Pauchard, M.; Huber, S.; Meallet-Rénault, R.; Maas, H.; Pansu, R.; Calzaferri, G. *Angew. Chem., Int. Ed.* **2001**, *40*, 2839−2842.

(6) Calzaferri, G.; Huber, S.; Maas, H.; Minkowski, C. G. *Angew. Chem., Int. Ed.* **2003**, *42*, 3732−2842.

(7) Gregg, B. A.; Resch, U. *J. Photochem. Photobiol., A* **1995**, *87*,157−162.

(8) Kresge, C. T.; Leonowicz, M. E.; Roth, W. J.; Vartuli, J. C.; Beck, J. S. *Nature* **1992**, *395*, 710.

(9) Inagaki, S.; Fukushima, Y.; Kuroda, K. *J. Chem. Soc., Chem. Commun.* **1993**, 680−682.

(10) Sasaki, M.; Osada, M.; Sugimoto, N.; Inagaki, S.; Fukushima, Y.; Fukuoka, A.; Itikawa, M. *Microporous Mesoporous Mater*. **1998**, *21*, 597−606.

(11) Murata, S.; Furukawa, H.; Kuroda, K. *Chem. Mater*. **2001**, *13*, 2722−2729.

(12) Tachibana, J.; Chiba, M.; Itikawa, M.; Inamura, T.; Sasaki, Y. *Supramolecular Sci*. **1998**, *5*, 281−287.

(13) Zhou, H. S.; Honma, I. *Chem. Lett.* **1998**, 973−974.

(14) Xu, W.; Guo, H.; Akins, D. L. *J. Phys. Chem. B* **2001**, *105*, 1543−1546.

(15) Armengol, E.; Corma, A.; Fornes, V.; Garcia, H.; Primo, J. *Appl. Catal. A* **1999**, *181*, 305−312.

(16) Takahashi, H.; Li, B.; Sasaki, T.; Miyazaki, C.; Kajino, T.; Inagaki, S. *Chem. Mater*. **2000**, *12*, 3301−3305.

(17) Yiu, H. H. P.; Wright, P. A.; Botting, N. P. *J. Mol. Catal. B: Enzymol*. **2001**, *15*, 81−92.

(18) Itoh, T.; Yano, K.; Inada, Y.; Fukushima, Y. *J. Mater. Chem*. **2002**, *12*, 3275−3277.

(19) Itoh, T.; Yano, K.; Inada, Y.; Fukushima, Y. *J. Am. Chem. Soc*. **2002**, *124*, 13437−13441.

(20) Causgrove, T. P.; Brune, D. C.; Blankenship, R. E. *J. Photochemem. Photobiol., B* **1992**, *15*, 171−179.

(21) Savikhin, S.; Buck, D. R.; Struve, W. S.; Blankenship, R. E.; Taisova, A. S.; Novoderezhkin, V. I.; Fetisova, Z. G. *FEBS Lett*. **1998**, *430*, 323−326.

(22) Bratt, P. J.; Poluektov, O. G.; Thurnauer, M. C.; Krzystek, J.; Brunel, L. C.; Schrier, J.; Hsiao, Y. W.; Zerner, M.; Angerhofer, A. *J. Phys. Chem. B* **2000**, *104*, 6973−6977.

(23) Itoh, T.; Ishii, A.; Kodera, Y.; Hiroto, M.; Matsushima, A.; Nishimura, H.; Inada, Y. *Res. Chem. Intermed*. **1996**, *22*, 129−136.

(24) Loach, P. A. In *Handbook of Biochemistry and Molecular Biology*, 3rd ed. Fasman, G. D., Ed. CRC Press: 1976; Vol. I, pp 122−130.